The effect of obtaining conditions on the structure and composition of Cu-MoS_2 coatings upon magnetron sputtering of composite targets.

A. Sagalovych, V. Popov, V. Sagalovych, S. Dudnik, A. Dzjuba.

Abstract. *The surface morphology and phase composition of the coatings obtained by magnetron sputtering of Cu-MoS_2 composite targets have been studied by X-ray diffraction, scanning electron microscopy and X-ray spectral microanalysis. X-ray diffraction studies of coatings show presence of two crystalline phases, namely Cu with face-centered cubic lattice and $CuMo_6S_8$ with a rhombohedral lattice. Studies of the surface morphology in Cu-$CuMo_6S_8$ coatings revealed two types of structures. One of the structures is realized in the form of globular formations, while the second is similar to the structure that had single-component Cu coating.*

X-ray spectral microanalysis showed that globular formations have higher Mo and S contents in comparison with other type of surface structure. The ratio between these elements is close to that in $CuMo_6S_8$. However, the Cu content is many times higher than the calculated amount for this compound. This suggests that globular formations are heterostructural where only one of the phases is $CuMo_6S_8$. Other possible phases in globular formations should be based on copper. The total area of globular formations in the coating increases with an increase in the proportion of MoS_2 in the composition of the Cu-MoS_2 sputtered composite target and strongly depends on the substrate potential.

Key words: magnetron sputtering, coatings, copper, molybdenum disulfide, structure, composition, Chevrel phases.

1. Introduction.

Materials based on molybdenum disulfides with copper are useful in a number of fields of science and technology. In addition to their traditional use as a material for tribological purposes, the use of these materials for sensors [1], electrodes for power supplies [2, 3] and a number of other applications is under study.

Depending on the field of application of materials based on molybdenum disulfides and its functional purpose, various methods of obtaining such materials can be used, namely chemical, electrochemical, metal Injection molding and some other methods. Certain properties of materials based on molybdenum sulfides are determined by their structure and composition, which, in turn, are very sensitive to the methods and conditions of their preparation. Depending on the method and conditions for the formation of materials based on molybdenum and copper sulfides, composite two-phase materials Cu-MoS_2 or compounds of $Cu_xMo_nS_{n+1(2)}$ type, where $0 < x<3,5$, $n=2$.[1-6].

Magnetron methods of pallet sputtering are among the methods used for synthesizing compounds of the CuxMonSn + 1 type (2) or the so-called Chevreul phases. [7-9]. The coatings obtained in these works were used as an object for studying superconducting properties of this type of compounds and effect of the ratio of the components of this compound on the value of the superconducting transition temperature. The composition of the coatings depended on the ratio of the areas of molybdenum disulfide and copper in the composite target of the magnetron sputtering source, and this was the main parameter that changed during the preparation of coatings. There were no specific values for the area ratio of molybdenum disulfide to copper disulfide in the composite target of the magnetron sputtering source. They were the first works devoted to obtaining coatings based on molybdenum and copper disulfides by the magnetron method.

Subsequently, most of the works was focused on obtaining coatings by the magnetron method based on molybdenum disulfides alloyed with other metals such as Ti, Zr, Cr, and their solid compounds, as well as Co, V, Fe, Ni and some others. The purpose of such studies was mainly to increase the wear resistance of materials based on molybdenum disulfide and to maintain high lubricating properties under operating conditions in humid air (10-14).

The variety of properties of compounds of molybdenum disulfides with copper and new possible fields of their use gave rise to broader study of the properties and methods of obtaining such compounds. This formed the basis for this work, the purpose of which was to study the effect

on the structure and composition of the conditions for obtaining coatings by magnetron sputtering of a composite target MoS_2 – Cu.

2. Equipment and study methods.

The experiments on the production of coatings were carried out in the Avinit M unit of the **Avinit** [a] automated vacuum-plasma depositing cluster based on upgraded unit УВН 71 equipped with a TORUS® 3" HV planar magnetron sputtering source with R601 high-frequency power supply provided by Kurt J. Lesker. MoS2 target manufactured by Kurt J. Lesker with a thickness of 6.3 mm and a diameter of 76 mm and disc of the same diameter made of copper of the M0 grade were used as target of the magnetron sputtering source. The composite target was represented by sandwich of MoS_2 disk and a copper disk with holes. The holes were located in a circle in the area of maximum target sputtering rate, limited by the radii R ~ 18 mm and R ~ 28 mm. Using copper targets with a different number of holes, and hence with different ratio of the surface area of the sputtered materials in a composite target, it was possible to obtain coatings of different compositions. High-voltage power supply up to 1.7 kV equipped with arc suppression system was used to ensure the potential on substrate.

Bronkhorst EL-FLOW PRESTIGE FG-201CV flow meter was used to supply process gases into the chamber as well and control and maintain gas flow rate at certain level. KPDR900 vacuum gauge provided by Kurt J. Lesker was used to control the pressure in the chamber, a . High-purity argon of grade A was used as process gas during the operation of the magnetron sputtering source. The unit is equipped with FTC 2800 thickness gauge provided by Kurt J. Leske in order to control the coating growth rate and determine the coating thickness online. The thickness could also be determined by height of the step formed during the growth of the coating on the substrate, part of which was masked. Under such method for determination of coating thickness, the height of the steps was measured using measuring station Hommel-Etamic Nanoscan 855 for controlling the roughness and surface contour.

X-ray structural studies of the coatings were carried out by means of ДРОН-2.0 diffractometer in filtered Cu-Kα radiation. X-ray diffraction patterns were recorded for phase analysis according to Bragg-Brentano's focusing scheme θ-2θ within angular range from 10 to 100 degrees.

After processing the diffraction patterns and determining the angular position of diffraction peak, the interplanar distance d_{hkl} was calculated using the Wolf-Bragg formula. The size of the coherent scattering regions in the samples (CSR) was determined based on broadening of diffraction lines using the Scherrer formula. The morphology and elemental composition of the coatings were studied using a scanning electron microscope РЭМ-106И with an X-ray energy dispersive analysis system [24].

The coatings were applied to substrates made of EI10 steel, which had been subject to surface cleaning after manufacturing using the technology adopted by FED JSC. Before placing the samples in the vacuum chamber, the surface of the substrates was additionally wiped with a coarse calico pad soaked in solvent gasoline in accordance with TU U22340203.001-97 (C2-80/120). After loading the substrates, the vacuum chamber was evacuated to the pressure of ($2.7 \div 3 \times 10^{-2}$ Pa). Then Ar was supplied through the flow meter at a rate at which the pressure in the chamber increased to ~ 6 Pa, and a negative voltage was applied to the substrate from a high-voltage rectifier for the purpose of cleaning the surface of the substrate in glow-discharge plasma. The voltage was gradually increased to 600V and once stable combustion of the glow discharge is reached without micro-arc breakdowns it was kept at this level for 5 minutes. After the completion of the ion-plasma cleaning of the substrate, the supply of Ar was reduced until the pressure was ~ 10^{-1} Pa, under which the discharge was ignited in the magnetron with closed shutter. During 5 minutes of operation of the magnetron, the discharge power was gradually raised to 200 W with a simultaneous decrease in the Ar flow rate until necessary pressure was reached in vacuum chamber, i.e. ($7 \div 8$) x10^{-2} Pa. The magnetron shutter was opened and coatings were applied on all samples studied in this work for 1 hour in this operation mode of magnetron.

3. Study results and discussion.

Preliminary studies were carried out to obtain coatings by the magnetron method through sputtering only molybdenum disulfide target and copper target in order to determine the growth rate and structural characteristics of such coatings for subsequent assessment of the effect on these characteristics of coatings obtained by sputtering a composite target. Experiments were also carried out to determine the minimum ratio of the surface of the sputtered materials in the composite target, at which the formation of sulfide phases in the coating could be detected by means of used study methods. Carried out studies have shown that such a minimum ratio of the sputtered surface of MoS_2 to Cu in the area of maximum target sputtering rate, limited by the radii R ~ 18 mm and R ~ 28 mm, is close to 0.4. Based on this fact, composite targets, in which the ratio of the area of sputtered surface of MoS_2 to Cu exceeded 0.4, were used .Considering this fact, composite targets, in which the ratio of the area of the sprayed surface of MoS_2 to Cu exceeded 0.4, were used in further studies.

X-ray diffraction analysis of coatings obtained by sputtering a copper target showed that only single phase, Cu, with an face-centered cubic arrangement is revealed. All the lines of this phase were present. The ratio of their intensities was close to the tabular values, i.e. there was practically no preferential orientation. Lattice spacing was equal to 0.3617 nm, which coincides within the error with the tabular value of 0.3615 nm. The size of the coherent scattering regions (CSRs) was 103 nm. The growth rate of the coating, measured with a thickness gauge and determined using a profilometer by step height, had approximately the same value and amounted to 4.26 μm/hour and 4.4 μm/hour, respectively.

Similar studies for coatings obtained by sputtering molybdenum disulfide target revealed the presence of only the hexagonal MoS2 phase. The film lines were weak and wide, suggesting finely dispersed crystal structure. The strongest reflection of this phase is MoS_2 (002) at the diffraction angle 2θ near 14.4 deg. was hardly visible due to formation of the texture. The line intensity ratio indicated that the coating had a texture with a predominant orientation of the crystallographic planes (101) parallel to the substrate plane, at which the axis of the hexagon c is tilted by 40 degrees to the film plane. The lattice spacing had the values a = 0.316 nm, c = 1.229 nm, which practically coincides with the table values for the MoS_2 lattice spacing a = 0.3161 nm and c = 1.2294 nm. The CSR size was 10 nm. The coating growth rate was 2.2 μm/hour.

When obtaining complex Cu–Mo–S coatings, two composite targets were used, in which the ratio of the sputtered surface of MoS_2 to Cu in the area of target maximum sputtering rate was 0.44 and 4. Coatings No. 1 were obtained by sputtering a composite target at ratio of the sputtered surface MoS_2 to Cu that was equal to 0.44 and in the absence of potential on the substrate. Coatings No. 2, No. 3, and No. 4 were obtained by sputtering a composite target at ratio of the sputtered surface of MoS_2 to Cu that was equal to 4 and at a negative potential on the substrate of 100 V and 200 V, respectively. The growth rate of coatings No. 1 was 3.25 μm/hour and growth rate for coatings No. 2 was equal to 3 μm/hour. The coatings that were deposited on substrates with a negative potential had noticeably slower growth rates. So, for coating No. 3 it was 1.58 μm/hour, for coating No. 4 it was 1.5 μm/hour.

X-ray diffraction analysis of coatings obtained by sputtering MoS_2-Cu composite target suggests the presence of two phases regardless of the relative fraction of the copper component in the total area of the composite target and the potential on the substrate. The main phase is Cu with face-centered cubic arrangement. The second phase, the lines of which are much weaker, is the rhombohedral $CuMo_6S_8$. The X-ray diffraction patterns also showed the lines of steel substrate made of the α-Fe. Table 1 shows the results of numerical processing of diffraction patterns: angular position $2\theta_{max}$, interplanar distance d, intensity I and half-width B1/2 for the first five diffraction lines present on diffraction patterns. Table 2 shows the integral intensities of the main reflections on diffraction patterns and the ratio between them for Cu and $CuMo_6S_8$.

Table 1.

Results of numerical processing of a portion of diffraction patterns.

No.	$2\theta_{max}$, deg.	d, 10^{-1}nm	I, c.u.	$B_{1/2}$, deg.	Phase
Sample No.**1**					
1	41.22	2.188	6	1.05	$CuMo_6S_8$
2	43.28	2.088	367	0.33	Cu
3	44.40	2.040	26	0.99	α – Fe
4	47.43	1.915	3	0.61	$CuMo_6S_8$
5	50.29	1.812	18	0.96	Cu
Sample No.**2**					
1	40.93	20.203	12	0.81	$CuMo_6S_8$
2	43.28	2.089	60	0.57	Cu
3	47.62	1.908	10	0.64	α – Fe
4	44.24	2.046	7	1.0	$CuMo_6S_8$
5	50.34	1.811	17	0.85	Cu
Sample No.**3**					
1	40.69	2.215	6	0.90	$CuMo_6S_8$
2	42.87	2.108	53	0.86	Cu
3	44.10	2.052	29	0.82	α – Fe
4	47.13	1.927	3	1.70	$CuMo_6S_8$
5	49.80	1.829	9	1.50	Cu
Sample No.4					
1	40.87	2.206	5	1.06	$CuMo_6S_8$
2	42.96	2.103	51	0.96	Cu
3	44.30	2.046	21	1.16	α – Fe
4	47.5	1.912	4	0.82	$CuMo_6S_8$
5	49.60	1.836	6	1.54	Cu

Table 2.

Integral intensities of the main reflections in diffraction patterns for Cu and $CuMo_6S_8$ and the relationship between them.

α – Fe	Cu				$CuMo_6S_8$			$I_{Cu}/I_{CuMo_6S_8}$
(110)	(111)	(200)	(220)	$I_{111}/ I_{200}/ I_{220}$	(131)	(042)	(431)	
Sample No.1								
24	147	20	10	100/13/7	10	2	0	14.7
Sample No.2								
5	41	17	9	100/41/22	11	5	3	3.3
Sample No.3								
22	50	14	4	100/28/8	6	5	1	5.6
Sample No.4								
23	54	9	4	100/17/8	8	4	0	5.6

The numerical criterion for the presence of texture is the deviation of the ratio of the intensity of diffraction lines from the values given in the database for a non-textured sample. For copper, the ratio of non-textured sample is $I_{111}/I_{200}/I_{220}$ = 100/46/20. From the data shown in Table 2, it can be seen that this ratio practically coincides with the data for sample No. 2. For the rest of the samples,

the (111) orientation prevails. The strongest reflection of the $CuMo_6S_8$ (101) phase at the diffraction angle 2θ near 13.8 was absent in the diffraction patterns, suggesting the presence of a texture for this phase. The ratio of the line intensities suggested that the $CuMo_6S_8$ compound in the coating had a predominant orientation of the crystallographic planes (131) in parallel to the plane of the substrate. Under such orientation of the planes, the axis of the unit cell c is located at an angle of 15 degrees to the plane of the film. The presence of texture makes it impossible to correctly perform quantitative phase analysis. Numerical criterion that characterizes the ratio of the phase content may be taken very roughly as ratio of the sums of the integrated intensities $I_{Cu}/I_{CuMo_6S_8}$ of all identified lines of the Cu and CuMo6S8 phases. The lower the ratio, the higher the content of the second phase. According to this criterion, the minimum content of $CuMo_6S_8$ was in sample 1, and the maximum one was observed in sample 2. Samples No. 3 and No. 4 had similar values for the $CuMo_6S_8$ content. More accurate data on the content of Cu in the coatings were obtained from the results of X-ray spectral microanalysis of these coatings. Thus, Cu content was 98.2 wt% in sample No.1, 87 wt% in sample No.2, 93.1 wt% in sample No.3 and 92 wt% in sample No.4.

Determination of the CSR value of the phases present in the coating (Table 3) showed that for Cu its value depends appreciably both on the content of the second phase in the coating and on the substrate potential. For the $CuMo_6S_8$ phase, CSR value of different coatings differs to a lesser extent. It can only be noted that presence of a potential on the substrate and its increase results in decrease of CSR value of this phase, as was the case for Cu phase.

Table 3.

Size of CSR phases disclosed in coatings.

Sample No.	CSR size, nm	
	Cu	$CuMo_6S_8$
1	40	12
2	23	16
3	15	14
4	14	12

Studies were carried out using scanning electron microscopy and X-ray spectral microanalysis (X-ray spectral microanalysis) in order to determine structural features of the surface of the obtained coatings,

The surface morphology of coating No. 1 differed from the coating obtained by sputtering a copper target, only by the presence of a small amount of precipitates. These precipitates were located mainly along cutter marks on the coating, which reproduced the morphology of the ground surface of the substrate and their size did not exceed fractions of a micron (Fig. 1). Elemental analysis in the area of such precipitates suggests, in addition to Cu, the presence of Mo in the quantity of 1.08 wt% and S in the quantity of 0.15 wt%. In the areas of the coating without precipitation, the Mo amount did not exceed 1 wt%. S was <0.1 wt%, i.e. threshold sensitivity of the system for energy dispersive analysis of X-rays or less.

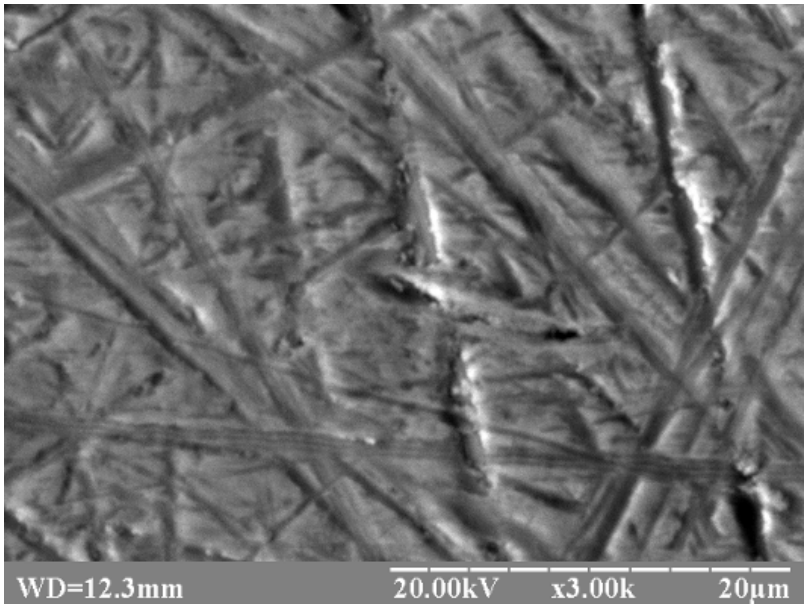

Fig. 1. Image of the coating surface of sample No. 1. The arrow indicates the precipitates, which were analyzed by EDX method.

The study of coatings No. 2-No. 4 revealed a strong influence of substrate potential on surface morphology. Figure 2 shows a view of the surface of the coating No. 2 obtained at zero potential of the substrate.

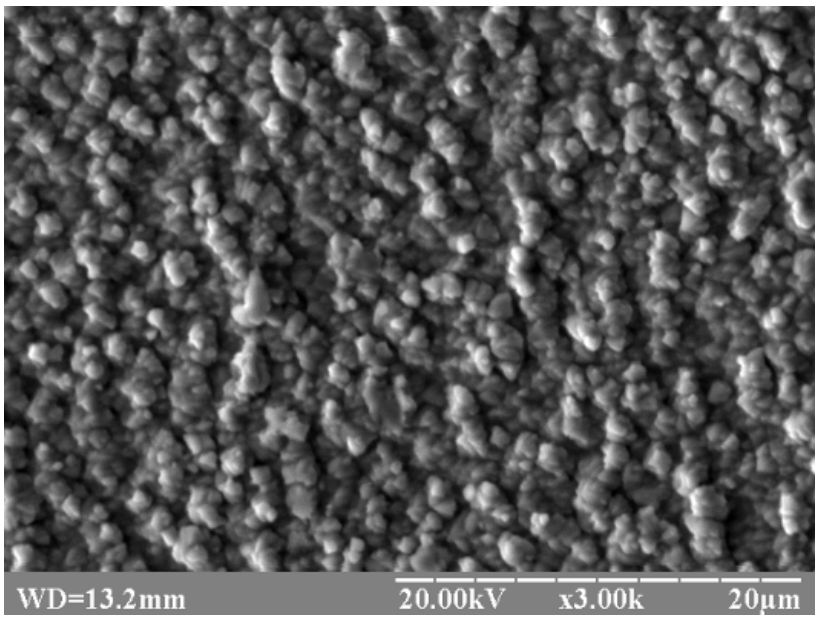

Fig. 2. Image of the surface of coating No. 2, obtained at zero potential of the substrate.

The coating has a homogeneous polydisperse globular structure with a maximum globule size of ~ 2 μm without reproducing the morphology of the ground substrate surface. The coating was gray. The average amount of Mo in globular formations was 8.81 wt%, and S was equal to 4.1 wt. %. The ratio of the amount of Mo and S, was 2, 15, which is close to the ratio of these elements in the compound $CuMo_6S_8$.

The image of surface of coating No. 3 obtained at a negative substrate potential of 100 V is shown on Fig. 3.

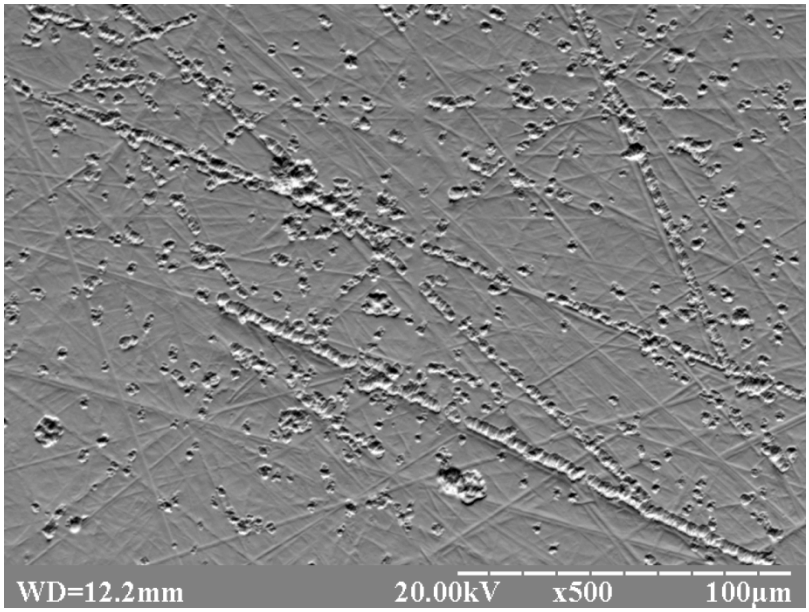

Fig. 3. Image of the surface of coating No. 3 obtained at a negative substrate potential of 100 V Arrows indicate the points at which the composition was analyzed by EDX method.

The coating had an inhomogeneous structure with globular precipitates that tended to form continuous chains along cutter marks on the coating, and there were also localized precipitates. The structure of this surface was, to some extent, similar to the structure of coating No. 1, not accounting amount and size of precipitates. According to the results of determination of composition of precipitates at points 1 and 2 by the XRD method, Mo content was equal to 13.37 wt. % and 6.67 wt%, S content was equal to 4.53 wt. % and 2.3 wt. %, respectively. The ratio of quantity Mo and S is 2.95 at point 1 and 2.9 at point 2. For $CuMo_6S_8$ of stoichiometric composition, the weight ratio of Mo and S is equal to 2.25. This means that the presence of the $CuMo_6S_8$ phase in the crystal lattice of this compound suggests the deficit of sulfur atoms. Determination of the composition of the coating in the interval between precipitates at point 3 suggests the presence of Mo in quantity of 6.8 wt% and S in quantity of 0.52 wt. %.

Surface structure of coatings obtained at a negative potential on the substrate of 200 V took intermediate position between the coatings for samples No. 1 and No. 3 (Fig. 4). The number of precipitates and their sizes were larger than for those of coating No. 1, but smaller compared to coating No. 3.

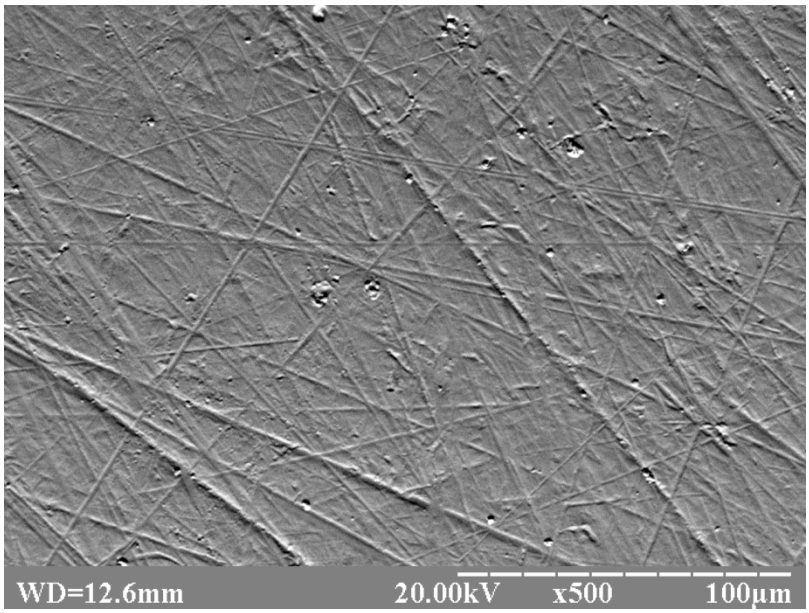

Fig. 4. Image of the surface of coating No. 3 obtained at a negative potential of substrate 155

V. The arrows indicate the points at which the composition was analyzed by the EDX method.

According to EDX data, the content of Mo was 14.04 wt. % and the content of S was 4.88 wt%. The size ratio of these elements in the inclusion was 2.88, which is quite close to the value of this ratio in inclusions of coating No. 3. In the interval between the inclusions (point 2 in Fig. 4), the coating contained Mo in quantity of 5.4 wt. % and S in quantity of 0.32 wt%. Studies of the surface morphology in Cu–$CuMo_6S_8$ coatings revealed two types of structures. One of the structures is realized in the form of globular formations, the second does not differ in appearance from the structure that had a single-component Cu coating. There is a definite correlation in in terms of quantitative ratio of such structures in the coating and the ratio of the intensities of the reflections $I_{Cu}/I_{CuMo6S8}$ on diffraction patterns (Table 2). Based on these facts, it could be assumed that the globular formations are presented by $CuMo_6S_8$ compound, and the second structure is Cu, which are recorded during X-ray diffraction analysis of these coatings. However, the data on the composition of these two types of structures do not allow such a conclusion. So, in the composition of the coating No. 2, which had a purely globular structure, besides Mo and S, there was Cu in quantity of 87 wt. %, which was many times higher than quality of this element in the $CuMo_6S_8$ compound. Since Mo/S ratio practically corresponded to the wt% ratio of these elements in the $CuMo_6S_8$ compound, it can be assumed that globular formations are heterostructural, where one of the phases is $CuMo_6S_8$. It is impossible to make certain assumptions regarding the composition of other possible phases in globular formations on the basis of obtained data, except that their base should be copper. In works Nos. [16, 17], coatings deposited by sputtering composite target Cu – MoS_2 through pulsed magnetron sputtering were also analyzed. The aim of these works was to obtain an antifriction material based on the Cu-Mo-S system with improved tribological characteristics. Despite the difference in the methods and conditions for obtaining coatings, the results presented in the work No. [16] and this paper have several common points regarding the composition and structure of the coatings. Studies in work No. [16] showed that the surface morphology of the coatings had two types of structures, although their appearance differed from the structures described in this work. Globular precipitates, determined by transmission electronic microscopy, consisted of a mixture of copper crystallites with an average transverse size of ~ 60 nm and sulfide nanoparticles $Cu_2Mo_6S_8$ with an average size of ~ 8 nm. The formations in the form of fibers had a nanocrystalline structure and consisted of the same sulfide nanograins that were present in the form of inclusions in globules. According to EXD data, the globules were present in the quantity of ~ 99 wt% (Cu), and the rest share was occupies by Mo and S in a ratio of ~ 0.7. Fibers were equal to 54.74 wt. % (Cu), 30 wt% (Mo) and 15.26 wt% (S). Testing such coatings in atmospheric area showed that they have significantly higher tribological properties compared to the matrix material free of sulfide inclusions. The mechanism of the formation of the $CuMo_6S_8$ phase, as well as heterostructural formations, observed in this work during magnetron sputtering of composite Cu-MoS_2 targets, is not clear. Minimum required concentration of all the components that make up the compound must be ensured for the formation of such compounds on the condensation surface of the coating. In this case, the minimum required concentration of only one or part of the elements included in the compound can be decisive. When sputtering MoS_2 targets by the magnetron method, the S content in the coatings, as a rule, turns out to be lower than it should be according to the stoichiometry for molybdenum disulfide. A decrease in S content in the coating was also observed upon increase in the temperature of the substrate, an increase in the negative potential of the substrate or the current density on the substrate [22.23]. This is due to the higher rates of re-evaporation and sputtering of S as compared to Mo.

In the coatings obtained in this work, the weight ratio of Mo to S was not less than 2.15, while for the sputtered target made of MoS_2 this ratio is equal to 1.5. This means that the concentration of S in the flow of sputtered target atoms was much higher than in the coating. If we proceed from the assumption that the S concentration on the growing surface is the minimum necessary for the formation of $CuMo_6S_8$, then this can be achieved starting only with a certain fraction of MoS2 in the sputtered target. This is conditioned by the fact that the $CuMo_6S_8$ compound was found in the coating only after the fraction of the MoS_2 surface in the sputtered composite target increased to a certain value. Due to change in the surface concentration of S, it is possible to explain the dependence of the number of globular formations on the potential of the substrate, which is associated with the presence of the $CuMo_6S_8$ phase in the coating. It is known that surface scratches are defects with increased surface energy, which makes adsorption of atoms on such defects energetically favorable. This means that the scratches will be in places with an increased concentration of S atoms. Therefore, the preferred formation of $CuMo_6S_8$ should have occurred precisely on such defects, which was observed in the study of the coating surface.

JSC FED widely uses various types of antifriction and wear-resistant coatings [18, 19] n the designs of aircraft units. They also include Cu-MoS_2 coatings obtained by the electrolytic method [20, 21]. Magnetron sputtering methods, in contrast to electrolytic ones, are environmentally friendly, low-waste coating methods, which makes their use preferable in industrial processes. In this regard, JSC FED sputtered $CuMo_6S_8$ coating by magnetron methods with total copper content of 87 wt% on parts, for which company's technology provide for deposition of Cu–MoS_2 (Fig. 5). The unit with a set of such parts has passed all trial operations and bench tests without any remarks. This fact confirms the possibility for using Cu-$CuMo_6S_8$ coating as an antifriction coating in one of the traditionally used field, where sulfide-containing coatings are used.

Figure 5. Set of parts with Cu – $CuMo_6S_8$ coating.

Conclusion.

The performed studies have shown that the structure and composition of the Cu-Mo-S coating

obtained by magnetron sputtering of MoS_2–Cu composite target depends not only on the composition of the composite target, but also very strongly depends on the substrate potential. Obtained results confirmed the possibility for synthesis of the Chevrel phase of $CuMo_6S_8$ by the magnetron sputtering method; however, the coatings obtained under the studied conditions were heterophase. X-ray diffraction studies, in addition to the $CuMo_6S_8$ phase, suggested presence of the Cu phase in all coatings. Studies of the elemental composition of areas with different types of surface morphology do not make it possible to unambiguously determine possible quantitative ratio of these phases. Nevertheless, the highest concentration of Mo and S with a ratio between these elements close to stoichiometric in the $CuMo_6S_8$ compound had globular formations on the coating surface.

List of references.

1. S. Boursicot, V. Bouquet, A. Bombard, et al., Electrochimica Acta, **257**, 436 (2017).
2. P.Saha, P. H. Jampani, M. K., Datta, et al., J.Electrochem.Soc., **161**, A593 (2014).
3. D. Muthuraj, S. Mitra, Mater. Res. Bull., **101**, 167 (2018).
4. Olivier Richard, Gustaaf van Tendeloo, et al., J. Electron Microsc. **49**, 493 (2000).
5. K.P. Furlan, J.D.B. de Mello, A.N. Klein., Tribol Int., **120**, 280 (2018).
6. Y. Zhang, S. Descartes, et al., J. Therm. Spray Technol., **25,**473(2016)
7. C. K. Banks, L. Kammerdiner, H. L. Luo., J. Solid State Chem. **15**, 271 (1975).
8. S. A. Alterovitz, J. A. Woollam, Phil. Mag B,, VOL. **40**, 497 (1979).
9. R. Ohtaki, B. R. Zhao, H. L. Luo, J. Low Temp. Phys, **54**, 194 (1984).
10. T. Gradt, T. Schneider**,** Lubricants, **4**, 32 (2016).
11. M. R. Vazirisereshk, A. Martini, et al., Lubricants, **7**, 57 (2019).
12. D.G. Teera, J. Hampshire, V. Foxa, V. Bellido-Gonzalez, Surf. Coat. Technol., **94-95,** 572 (1997).
13. N.M. Renevier, V.C. Fox, et al., Surf. Coat. Technol., **127,** 24 (2000).
14. X. Ding, X.T. Zeng, et al., Surf. Coat. Technol., **205**, 224 (2010).
15. Y. Man, Z, Guojun et al., Appl. Surf. Sci**., 36730,** 140 (2016).
16. S. Yu. Zharkov, V. P. Sergeev, et al., in: Book. High technologies in modern science and technology, Tomsk, Russia (2015), p. 394.
17. S. Yu. Zharkov, V. P. Sergeev, et al., J. Phys.: Conf. Ser. **1281,** 012096 (2019).
18. A. Sagalovych, V. Sagalovych, Tribol. Ind. Vol. **35**, 261 (2013).
19. A. Sagalovych, V. Popov, et al., East.-Eur. к. Enterp. Technol, **2**,6 (2020).
20. V. Tsyuryupa, E. Satanovsky, Bull. KhNAHU, **51,** 78 (2010).
21. C. Kerr, D. Barker, F., et al., Trans IMF*,* **78**, 171 (2000).
22. J. Moser, F. Lévy, J. Vac. ScI. Technol. A **12**, 494 (1994).
23. J. Wanga, W. Lauwerens, et al., Surf. Coat. Technol., **139,** 143(2001).
24. Reference to Stelmakh.